MDPI

Article

Viable Use of Tire Pyrolysis Oil as an Additive to Conventional Motor Oil: A Tribological and Physical Study

Abdullah A. Alazemi [1],*, Abdullah F. Alajmi [1] and Sultan M. Al-Salem [2]

1 Mechanical Engineering Department, Faculty of Engineering and Petroleum, Kuwait University, Kuwait City 13060, Kuwait; abdullah.alajmi1@ku.edu.kw
2 Environment & Life Sciences Research Centre, Kuwait Institute for Scientific Research, Kuwait City 13109, Kuwait; ssalem@kisr.edu.kw
* Correspondence: a.alazemi@ku.edu.kw

Abstract: Stockpiled end-of-life tires (ELTs) pose a serious environmental concern. In the current investigation, ELT pyrolysis oil (i.e., pyro-oil) was studied as a potential additive to conventional motor oil. The pyro-oil samples were mixed in different concentrations of 10 to 50 wt.% with commercial virgin motor oil to obtain a lubricant mixture. Chemical analyses were performed for the tire-recycled derivative material, as a potential route to utilize pyro-oils, valorize ELT waste, and reduce production costs of motor oil lubricants. Rheological examinations were performed to explore the impact of the pyro-oil on the rheological properties of the motor oil under several shearing rates and temperatures. Tribological analyses of the lubricant mixtures and the pure motor oil were accomplished to study the influence of the pyro-oil additive on the tribological behavior of motor oils. Lastly, thermal stability and wettability examinations were executed to assess the thermal and wetting properties of lubricant mixtures. The obtained results showed that adding a low concentration of the pyro-oil ($\leq$10%) will sustain the motor oil's chemical, wettability, thermal stability, rheological, and tribological properties, signifying a viable application of recycled ELTs and helping to reduce their environmental and economic impact. These findings offer a feasible route of use in the future to obtain low-cost oils with market specifications, utilizing pyro-oil as a sustainable and environmental oil additive.

Keywords: recycled tires; pyrolysis process; oil additives; viscosity; friction; wear

1. Introduction

Lubricants and mineral and motor oils have been used in numerous systems and industrial applications including compressors, pumps, motors, turbines, hydraulics, etc. The rheological and tribological properties of oils are key parameters and are considered to be the proper approach to quantitatively assess their performance [1]. Mineral oils comprise a complex blend of hydrocarbons (HCs) with a variety of additives. Aliphatic HCs are typically the most prominent ones in such mixtures. The source of the oil is also important in identifying its ultimate pollution potential, whether it be an industrial or automotive (used) oil [1,2]. Globally, Asian markets have the highest demand (30%), while North America and Western Europe have a demand of about 22 and 13%, respectively [3]. This is also in parallel with the differences in population and automobile vehicle availability. It is estimated that about 0.7 million tons per annum, making up 23% of the collected lubricant oil in Europe post-consumption, is illegally disposed of or burnt in an environmentally unsound manner [4]. Furthermore, 5.7 million tons are the estimate of lube oil consumption annually in Europe, with the major market share comprising the industrial and automotive

sectors [3]. On the other hand, the Middle-East has a total demand share of the lubricant market of 10% [5].

The utilization of oils has also become an important environmental concern over time, namely in terms of recycling lubricating oils, which could be conducted using various methods such as re-refining, reprocessing, or reclamation [6]. Readers are referred to Kupareva et al. [3] for more details on the different re-refining processes available on the market. Although energy consumption is projected to double by 2030 [7], the lubrication industry has demonstrated an increased attention to 'drop-in' fuels that are comprised of chemical and compositional properties comparable to traditional fossil fuels [8]. However, creating economically viable sustainable and renewable fuels capable of substituting traditional ones while maintaining a similar performance is a significant challenge. Furthermore, such products should also meet market specifications and environmental standards.

The transportation sector is interested in further investigating the applicability of oil lubricants extracted via different technologies, particularly using municipal solid waste and biomass [9,10]. End-of-life tire (ELT) waste is a good illustration of a distinct waste type that presents a hazardous environmental potential if not handled appropriately [11]. Additionally, ELT waste is known to have highly energetic components because of its petrochemical origin [12,13] and can deliver high-quality oils when processed by the pyrolysis technique [14]. The pyrolysis process has been gaining attention as a method to valorize numerous solid waste materials because of its energy balance and manageable operating parameters that can yield lucrative oils, mimicking crude oils [9]. ELT pyrolysis oil comprises aliphatic compounds, aromatic mixtures, impurities (PAH, S, and N mixtures), and more [15]. Nonetheless, the literature is lacking (and consequently, investigated in this study) a comprehensive study for the potential of utilizing pyrolysis oil (i.e., pyro-oil) as an additive to conventional motor oils. It is essential to examine the tribology of the pyro-oils obtained to be able to determine the main properties related to wear, friction, and lubrication with interacting surfaces. This will ultimately enable us to determine the role of such oils in mechanical systems during surface contact [16], which is responsible for about 23% of the energy loss in such mechanical systems [17]. Therefore, the related lubrication properties are also essential to determine the reduction in friction and wear damage [18]. Valorizing and recycling the rubber component from ELTs is considered to be a crucial strategy in implementing the UN sustainable development goals, namely for 'responsible consumption and production' goal number 12.

Lubricants are typically petroleum-based, containing about 90% mineral oils, while the rest is made of additives to increase lubrication and reduce friction [19]. Alazemi et al. [20] investigated tire pyrolysis oil's chemical, physical, and lubrication properties. They revealed that ELT pyro-oil demonstrated lower thermal stability, rheological, and wettability properties relative to a reference motor oil. Yet, the chemical structure and tribological behavior of the tire pyro-oil were similar to the reference motor oil. Nonetheless, a gap exists in the current literature regarding the effect of adding produced ELT pyro-oils to conventional motor oils and determining the impact of such a practice on the rheology and tribology behavior of the mixtures. Not only will such a practice provide a route to rid the environment of potential ELT accumulation, but it could also provide a new market for an industry when the studied properties are shown to be viable. In this research, we conducted a study dedicated to identifying the effects of the addition of pyro-oil derived from ELTs on conventional motor oil's lubrication and tribological performance. Pyro-oil acquired from ELTs was mixed in different concentrations between 10 and 50 wt.% with motor oil to obtain a lubricant mixture. Chemical analyses of the tire pyro-oil, motor oil, and other lubricant mixtures were conducted to explore and compare their chemical compositions. Furthermore, rheological analyses were implemented to understand the consequence of

pyro-oil addition on the rheological properties of the motor oil at different temperatures and shearing rates. Finally, tribological analyses were executed on the lubricant mixtures and the pure motor oil to assess the influence of pyro-oil on the tribological performance of motor oils.

2. Materials and Experimental Methods

2.1. Samples Preparation

The ELT pyro-oil sample was acquired from a fixed bed pyrolysis operation using ELTs retrieved and sourced from the State of Kuwait's commercial and municipal sources. The oils were produced at a temperature of about 500 °C, as described in [14]. The samples derived from this operating temperature were advantageous to carry out the work described herein, as the temperature of 500 °C was the highest pyro-oil-yielding operating temperature [14]. A total oil yield of $\approx$ 45% was obtained from the treatment of 0.2 kg feedstock with aluminum oxide packing. Approximately 90% of the obtained samples comprised hydrocarbons in the C_{12}–C_{20} compound range. The atomic balance on the employed reactor revealed that the feedstock was comprised of (g) carbon (C) 164.51, hydrogen (H_2) 17.39, nitrogen (N_2) 0.33, and sulfur (S) 6.28. The produced oil was comprised of (g) C 80.39, H_2 13.98, N_2 0.06, and S 0.30 [14]. The reference (virgin) motor oil (5W-30 motor oil) used in this study was sourced from Valvoline Company in the United States. The pyro-oil sample was mixed with the motor oil in three different ratios, as per the following (pyro-oil/motor oil-wt/wt%): 10/90, 30/70, and 50/50. The pyro-oil was mixed with fully formulated oil (5W-30) in order to demonstrate the feasibility of utilizing pyro-oil in the oil lubricants industry. Direct sonication for 120 s using an ultrasonic horn processor (Misonix, model S-4000-010, Farmingdale, NY, USA) at a power altitude of 20% was used to prepare the pyro-oil/motor oil mixtures at different weight percentage concentrations. Figure 1 shows the samples before and after mixing and sonication. The yellowish appearance visible to the naked eye is an indication of the cracking of higher HCs. Before sonication, a clear layer was noticeable to the naked eye with the lower pyro-oil concentrations, indicating a variation in density and physical properties. However, a uniform and homogenous mixture was achieved after sonication and maintained its homogeneity for several days.
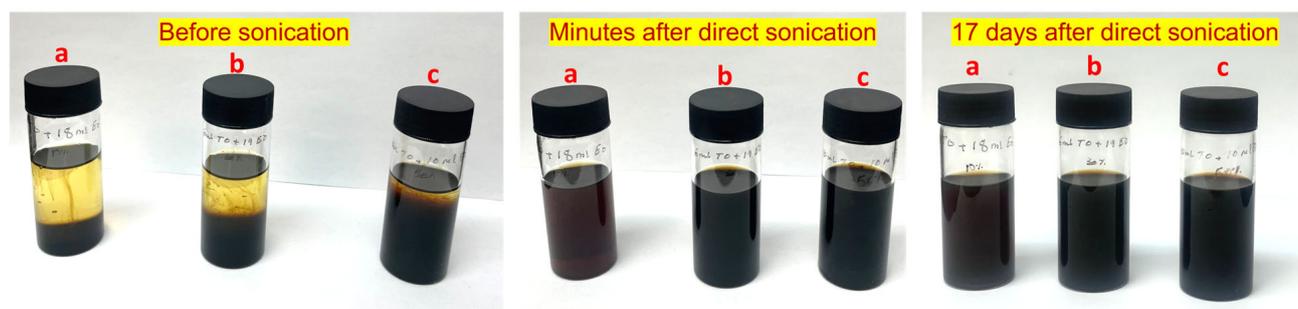
Figure 1. Mixed samples used in this work (pyro-oil/motor oil—wt./wt.%): (**a**) 10/90, (**b**) 30/70, and (**c**) 50/50, showing the effect of sonication and settling for seventeen days.

2.2. Characterization Methods

Elemental (C, H, N, and S content) chemical studies were estimated via a Vario Macrocube Analyzer (Elementar, Frankfurt, Germany) using dynamical combustion in order to decompose the examined materials into simple compounds ($\geq$1050 °C). The gaseous sample is sent to a chromatography column using helium gas as a carrier. The obtained products are in the form of CO_2, H_2O, N_2, and SO_2. Lastly, the fluid flow arrives at the gas chromatographic column that guarantees a homogenous and modular temperature, causing the elements to separate and finally identifying C, H, N, and S elements using

a thermal conductivity detector (TCD). An X-ray fluorescence (XRF) apparatus, Rigaku ZSX, Primus IV (Rigaku, Tokyo, Japan), equipped with a 4 kW Rhodium tube was used to quantitatively determine the atomic elements in all oil samples. A liquid sample of 5 mL was used in the XRF analysis for each experimental run. The thermal stability was determined as described by the ASTM-E2550(ASTM E2550-17; Standard Test Method for Thermal Stability by Thermogravimetry. ASTM International: West Conshohocken, PA, USA, 2017) via a thermogravimetric analyzer (TGA) apparatus (Mettler Toledo, model TGA2, Columbus, OH, USA). Prior to testing, the chamber in the TGA apparatus was purged using dry air for 60 min. Subsequently, a 70 μL platinum crucible pan was used to hold about 10 mg of the examined oil sample in the TGA apparatus. Then, the thermal stability study was performed by elevating the sample's temperature from 25 °C to 600 °C using a 10 °C per minute heating rate through nitrogen gas at 50 mL per minute flow rate.

The viscosity and rheological behavior of the motor oil, pyro-oil, and their mixtures were determined using a TA Instruments ARES-G2 Rheometer (New Castle, DE, USA), using concentric cylinders set up with an oil sample of 10 mL in every test. The dynamic viscosity was measured under a temperature rise from 5 to 60 °C for the oils and their mixtures using a constant shear rate of 5 per second. Furthermore, viscosity measurements for oil samples were performed at different temperatures of 25, 50, and 75 °C for a shear rate of 1 to 100 per second. The structure of molecules in each oil sample was examined by running Fourier Transform Infrared Spectroscopy (FTIR) to quantitatively obtain minor and major atomic elements. The IR spectrum acquired for all oil samples was performed for a wavenumber $(1/\lambda)$ in the range of 500 to 4000 cm^{-1} according to the study conducted by Decote et al. [21]. The wettability examination of all oil samples was performed using a contact angle goniometry instrument (Dataphysics, model OCA100, Filderstadt, Germany) according to the technique described by Alazemi et al. [22], utilizing a 5×5 cm stainless steel substrate, which was placed in the goniometer instrument, and the contact angle (CA) was measured at different temperatures (25, 50 and 75 °C). The CA was measured on the polished stainless steel substrate through the instrument's software(SCA-20 Software, version 4).

The lubrication of oils is pivotal in reducing wear and controlling machinery friction [23]. Therefore, a Tribometer (Rtec instruments, model MFT-5000, San Jose, CA, USA) was employed to perform tribological examinations of all examined oils using 10 mL samples at different operating temperatures (25 °C, 50 °C, and 75 °C). The investigated temperatures were selected because the operating temperature of oil lubricants in most industrial applications ranges between 40 and 80 °C [24]. Tribotesting was performed using a ball-on-disk setup and following the ASTM-G99 standards. A 20 N normal force (F_N) was applied in each tribotest on a fixed 9.5 mm diameter E52100 alloy steel ball in contact with a 50 mm diameter stainless steel disk resulting in a maximum contact stress of 1300 MPa. This extreme contact stress of the ball-on-disk configuration ensures that the examined oil sample is studied in boundary and mixed lubrication situations [25]. The steel disk rotates with a speed (ω) ranging from 0 up to 1500 rev/min. This ball-on-disk setup in the tribotests was set at a sliding diameter of 25 mm. In all tribotests, the tribometer instrument was stabilized at the chosen temperature for 60 s. Next, the rotational speed was increased to 1500 rpm in 120 s. Then, the rotational speed was decreased in several steps to evaluate the oil's lubricant behavior in different lubrication conditions. The time of each step was 120 s and the total tribotesting time was 4440 s. The friction coefficient (COF) was measured and used to generate a Stribeck curve to assess the lubricating property of the examined oil samples. Following every tribotest, the disk and ball wear scars were inspected via a profilometer at 10 and 20× magnifications. Multiple tests were conducted

to confirm the accuracy and consistency of the experimental outcomes, and the obtained results were within a 5% error limit.

3. Results and Discussion

3.1. Elemental Composition and FTIR Analysis

The elemental composition is presented in Table 1, whereby the ELT pyro-oil sample displayed a carbon content of about 48%, agreeing with the atomic balance of the oil sample [14]. The results revealed that the pyro-oil/motor oil mixtures showed a similar oxygen content compared to the virgin motor oil (see Table 1). Moreover, it is common to observe slight deviations in pyrolysis oils with time caused by oxidation [26]. The motor oil displayed a carbon content of approximately 50% (see Table 1), and there was no significant carbon content change for the pyro-oil/motor oil mixtures. Nonetheless, a clear difference in sulfur content was observed (Figure 2). The motor oil had a 0.31% sulfur content, while the pyro-oil had more than double the sulfur amount (0.71%), whereas the mixtures ranged between 0.34 and 0.42%. Pyro-oil showed a similar sulfur range to past investigations on thermal and catalytic pyrolysis samples [27,28], and the motor oil when compared to both used and fresh lubrication oils [1]. The high sulfur content in the pyro-oil compared to engine oil is attributed to the tire's vulcanization process during the manufacturing of tires. Further elemental analysis was performed using the XRF instrument; the results confirmed that carbon and sulfur are the main elements in the ELT pyro-oil sample and no inorganic components were detected (see Table 2). The XRF analysis of the pyro-oil was quite distinctive compared to standard motor oils [29].

Table 1. Results of elemental analysis for tested oil samples.

Sample (wt./wt.%)	Nitrogen (N, %)	Carbon (C, %)	Hydrogen (H, %)	Sulfur (S, %)	Oxygen (O, %)
Motor Oil	0.065	50.385	16.746	0.310	32.49
ELT Pyro-Oil	0.415	47.890	11.754	0.7165	39.22
ELT Pyro-Oil/Motor Oil (10–90%)	0.075	50.465	16.885	0.342	32.23
ELT Pyro-Oil/Motor Oil (30–70%)	0.165	51.575	14.740	0.390	33.13
ELT Pyro-Oil/Motor Oil (50–50%)	0.215	50.965	13.209	0.424	35.18
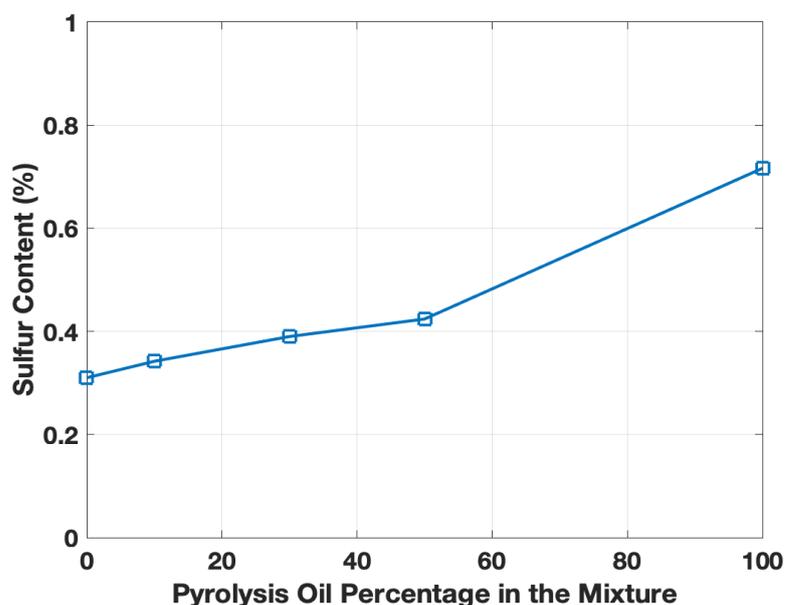
Figure 2. Sulfur content as a function of ELT pyro-oil content (wt.%) in motor oil.

Table 2. XRF analysis parameters of the pyro-oil sample utilized in this study.

No.	Element	Outcome (Mass%)	Det. Limit	El. Line	Intensity	w/o Normal
1	Si	0.0000	0.01059	Si-KA	0.1744	0.0000
2	P	0.0601	0.00168	P-KA	9.2321	0.0601
3	S	0.5680	0.00150	S-KA	92.0354	0.5678
4	Ca	0.0131	0.00117	Ca-KA	1.8046	0.0131
5	Br	0.0005	0.00022	Br-KA	4.0943	0.0005
6	C	99.400				99.3585

The 10% addition of ELT pyro-oil had a minimal impact on the sulfur content, which points towards prioritizing it as a prime product and a candidate to utilize in the future as part of the manufacturing cycle. In addition to the environmental benefits linked with chemically recycling the ELTs, the 10% pyro-oil mixture also presents itself as having an added value to reduce costs and have additional pathways of utilization for such products. This is especially true when considering the tribological properties (discussed later on) and physical appearance of the mixture, which is close and similar to that of motor oil. The mixture mentioned above (i.e., ELT pyro-oil/motor oil 10–90%) also showed a similar oxygen content compared to the virgin motor oil (see Table 1), which was evaluated by subtraction. The similar oxygen content in both oil samples implies that they have comparable calorific values (CVs) and a higher one relative to the ELT pyro-oil [30].

The FTIR signals of the examined specimens are recorded and shown in Figure 3. The 10–90% mixture showed a clear similarity to that of the virgin motor oil, indicating almost no chemical print impact when a minimal addition of the ELT pyro-oil is applied (e.g., 10 wt.%). Other similarities in the obtained spectrums were noted for the other examined specimens. The displayed and studied spectra result from the vibration of functional groups, which are presented as a function of wavenumbers. In theory, a nearby 3000 cm^{-1} frequency suggests an aliphatic alkane (C-H stretching) group [27]; this was fairly evident in the examined oil samples. A detected peak at 2726 cm^{-1} was quite prominent in the case presented at hand (Figure 3).
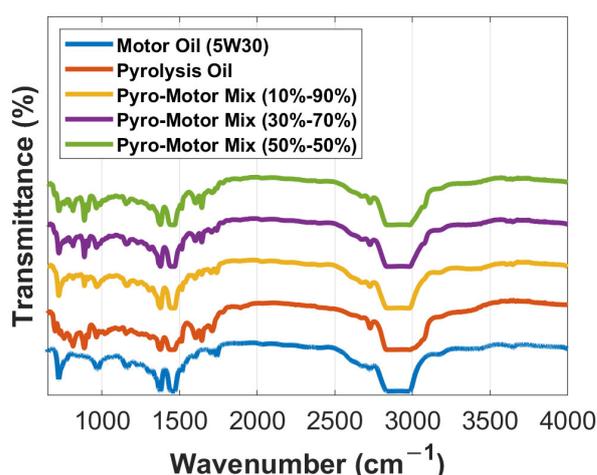
Figure 3. Comparison of FTIR transmittance spectrum for the pyro-oil, motor oil, and their mixtures.

There were no signs of alkene C-H stretching groups observed for the pyro-oil samples at a wavenumber of more than 3000 cm^{-1}, which was a distinctive feature of the motor oil. A similar finding was recorded by Osayi et al. [31] for two oil samples obtained via the pyrolysis process of natural rubber and ELTs. For the motor oil sample, the actual peak

was detected near 3700 cm^{-1}. Both CH$_2$ and CH$_3$ bending were hardly measurable in all examined oil samples. Unlike the motor oil, the pyro-oil sample demonstrated the existence of an obvious C=C stretching aromatic ring with a 0.18 intensity. This was marginally measurable in the equivalent functional group scope (Figure 3). Also, the aromatic rings (C=C) were observed more obviously in the pyro-oil sample in the 900 to 690 cm^{-1} range. Particularly, the aromatic rings were noticed at nearly similar peaks in all oil samples at 698, 758, 814, 887, and 911 cm^{-1} frequencies. This is a clear indication that the pyro-oil sample's aromaticity is greater than that of the examined motor oil. ELTs comprise monoaromatics such as limonene and isoprene [14,28], which can lead to such observations. An additional vibration was noted with the pyro-oil sample towards 3650 cm^{-1}, which is a clear indication of H-O-H water molecules [32,33]. More sulfur contamination was evident for the pyro-oil sample (1150 cm^{-1}), which is logical due to its origin when compared to the motor oil sample and its mixtures.

Furthermore, it should be noted that at 1710 cm^{-1}, a peak was observed in pyro-oil sample and was correlated with carbonyl groups (C=O in stretching), which was not noticed in the motor oil sample. This might be due to the oxidation of the oil sample over time and storage. Aldehydes/ketones or amide groups (1643 cm^{-1}) were detectable in the samples, although they were more obvious in the motor oil sample (see Figure 3). This finding was previously noted by several studies performed on ELT oils [31,34]. The motor oil additionally exhibited an N-H stretching functional group spotted around 3700 cm^{-1} related to acid chlorides. In addition, acid chlorides (C-Cl, 758 cm^{-1}), sulfonyl chlorides (S=O, 1377 cm^{-1}), and sulfonamides (N-H, 1515 cm^{-1}) were detectable in the pyro-oil sample, agreeing with prior results [14]. The dual peak profile and peaks adjacent to 500 cm^{-1} (alcohols, carboxylic acids, ethers, and esters) are frequently recorded and correlated with aromatics in different pyro-oils derived using various feedstock materials such as ELTs [30,35].

3.2. Thermal Stability

Thermal stability is a key property, specifically when the oil is utilized as a liquid lubricant under high operating temperatures. The thermal stability of oil lubricants is typically affected by their chemical structure. Oils' thermal stability is identified by the onset temperature (T$_{on}$), which represents the temperature when the oil starts to decompose. This thermal decomposition includes a mass variation from the original reference mass [36]. The thermal stability analysis of the tested specimens is shown below until the end set temperature (T$_{end}$) of the thermograms at 600 °C (Figure 4). Figure 4a depicts TGA results comparing the percentage of mass change against temperature for motor oil, pyro-oil, and their mixtures. As shown in Figure 4a, the mass change profiles of all oil samples involve three different phases. In phase I, a small mass decrease of around 1% occurred for all oil samples. This temperature, associated with the 1% mass drop, is referred to as T$_{on}$ [37]. In phase II, the mass loss of all oil samples is rapidly occurring at a higher rate. The midpoint temperature represents the temperature at which the percentage of mass change reaches 50% of the original mass. In phase III, the rate of mass change declines until it reaches an almost plateau line with the remaining small amount of residual mass. The acquired TGA outcomes reveal that the motor oil has superior thermal stability relative to other oil samples. The decomposition of motor oil started at T$_{on}$ of 208 °C. The pyro-oil exhibited the worst thermal stability compared to other oil samples with a T$_{on}$ of only 61 °C. However, the 10–90% mixture demonstrated comparable thermal stability relative to the motor oil, as depicted in Figure 4a.
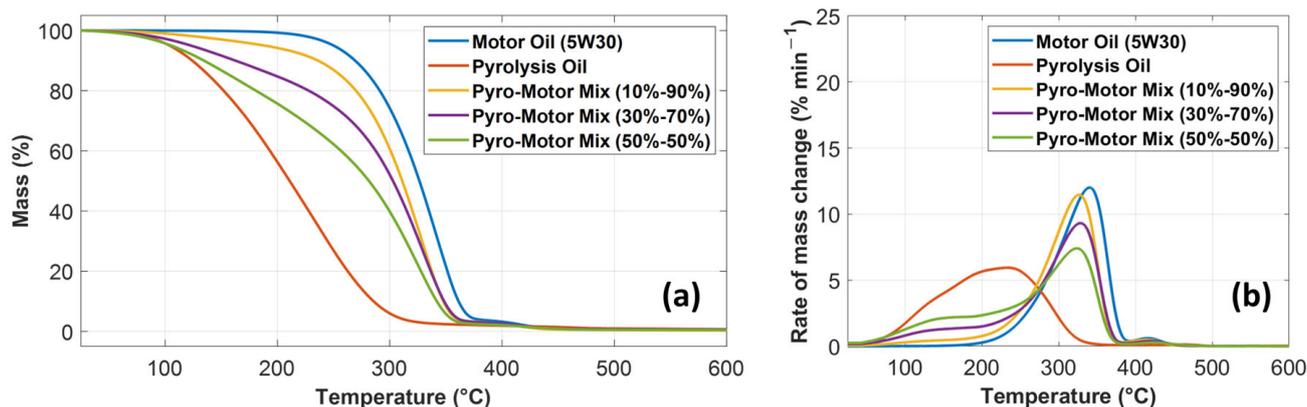
Figure 4. Comparison of (**a**) mass loss profile and (**b**) differential mass loss profile against temperature for motor oil, pyro-oil, 10–90% oil mixture, 30–70% oil mixture, and 50–50% oil mixture.

Figure 4b characterizes the derivative of the TG profile (DTG) relative to time for motor oil, pyro-oil, and their mixtures. In the DTG profile, the temperature associated with the maximum rate of mass change is referred to as the maximum temperature. Subsequently, the rate of mass change starts to decrease until it reaches a plateau line. From the DTG profiles, the motor oil clearly had the best thermal stability compared to other samples. However, the 10–90% mixture exhibited similar thermal stability behavior relative to the motor oil (see Figure 4b).

A summary of the acquired TGA data for all studied oil samples is shown in Table 3. It should be noted that the percentage of mass loss given in Table 3 signifies the mass loss (%) at the end of phase II. The onset temperatures of the motor oil, pyro-oil, and the 10–90% mixture are 208 °C, 61 °C, and 100 °C, respectively. The majority of industrial systems use lubricating oils at an operating temperature between 40 °C and 80 °C [24]; therefore, using pyro-oil as an oil lubricant in many industrial systems is problematic. However, the 10–90% mixture can be suitable as an oil lubricant for most industrial systems, since it has an onset temperature of 100 °C.

Table 3. Summary of thermogravimetric analysis results for motor oil, pyro-oil, and their mixtures.

Parameter	Motor Oil	Pyro-Oil	10–90% Mixture	30–70% Mixture	50–50% Mixture
Mass loss (%)	96.6	98.1	97.0	97.1	97.7
Onset temperature (°C)	208	61	100	71	63
Midpoint temperature (°C)	326	211	311	303	281
Maximum decomposition rate temperature (°C)	340	233	327	328	324

3.3. Rheological Analysis

An investigation of the rheological properties of pyro-oil/motor oil mixtures at different concentrations was executed and compared to motor oil at various temperatures and shearing rates. Figure 5 shows the viscosity variation with the shear rate for motor oil, pyro-oil, and their mixtures at different examined temperatures. The results showed that all samples' viscosity was almost constant at different shear rates, indicating their Newtonian behavior. Furthermore, the pyro-oil viscosity was found to be more than one order of magnitude lower than the viscosity of motor oil. However, the 10–90% oil mixture had a similar viscosity to motor oil for all shear rates and temperatures, implying that a low concentration of pyro-oil in motor oil has not affected the lubricant's viscosity performance.

Notably, the 30–70% oil mixture and the 50–50% oil mixture were 60% and 80% lower in viscosity than the virgin motor oil, respectively.
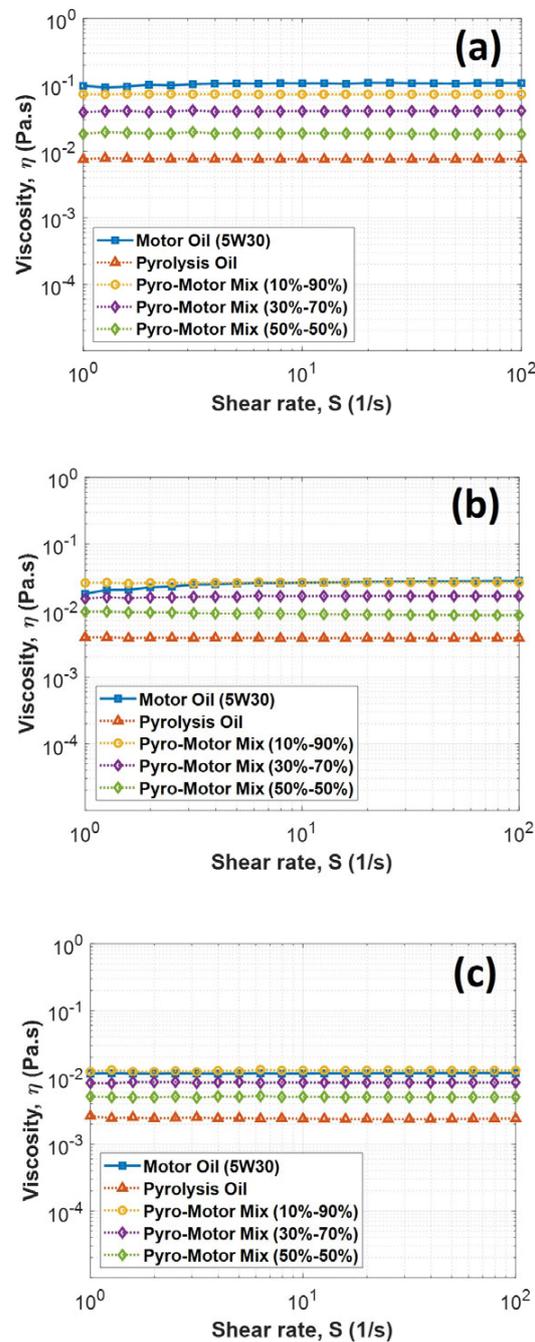
Figure 5. Variation in viscosity with shear rate for motor oil, pyro-oil, and their mixtures under examined temperatures of (**a**) 25 °C, (**b**) 50 °C, and (**c**) 75 °C.

Additional rheological analyses were performed to study the change in shear stress with shear rate under various temperatures for all samples. The obtained results indicated that shear stress is linearly proportional to shear rate for all oil samples and under all examined temperatures, as shown in Figure 6. Also, it was found that the motor oil and the 10–90% oil mixture had similar behavior at all examined temperatures and shearing rates, while the pyro-oil exhibited the lowest shear stress relative to other oil samples. Additionally, the 30–70% and 50–50% oil mixture results clearly indicate that adding a high percentage of pyro-oil to the motor oil will lower its viscosity and shear stress.
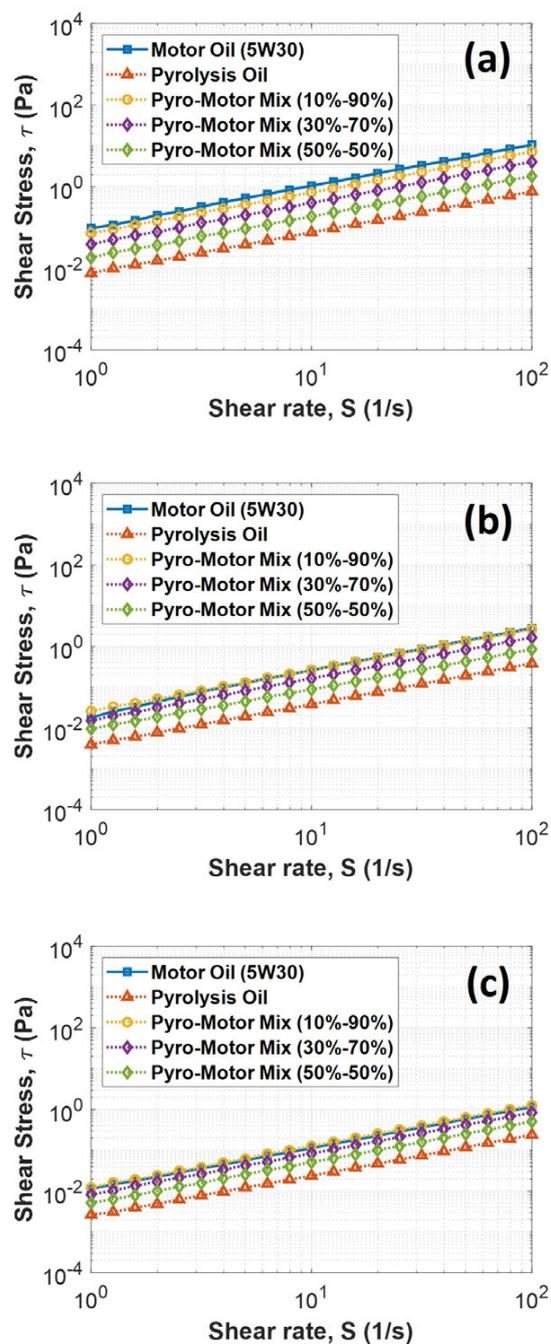
Figure 6. Variation in shear stress with shear rate for motor oil, pyro-oil, and their mixtures under examined temperatures of (**a**) 25 °C, (**b**) 50 °C, and (**c**) 75 °C.

An investigation of the change in viscosity with temperature at a constant shear rate was accomplished for all oil samples (Figure 7). It is clear that the pyro-oil's viscosity was less than the motor oil and other oil mixture samples under all examined temperatures. Furthermore, as the temperature becomes closer to 60 °C, the viscosity measurements of pyro-oil start to fluctuate, which could be explained by the fact that the onset temperature of pyro-oil is 61 °C, as discussed earlier. Compared to other oil mixtures, the 10–90% oil mixture exhibited a closer viscosity behavior to motor oil with a 35% maximum difference at all temperatures.
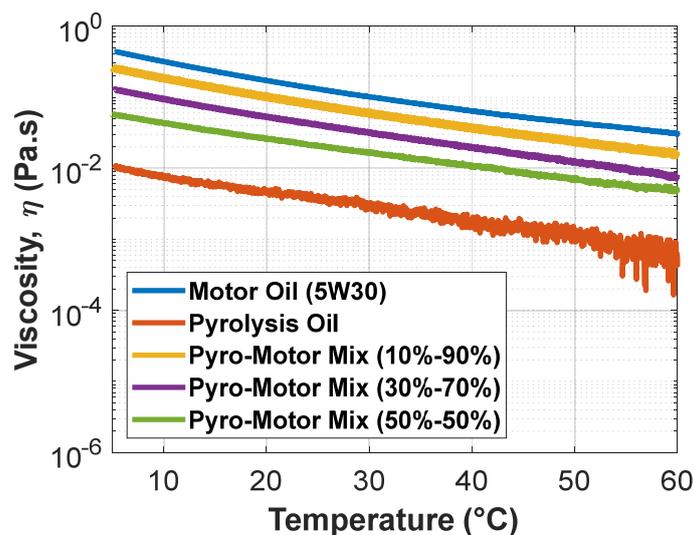
Figure 7. Variation in viscosity with temperature for motor oil, pyro-oil, and their mixtures.

The rheological results clearly demonstrate that adding a small concentration (less than 10%) of pyro-oil to the motor oil will have an insignificant effect on the motor oil's rheological performance. Therefore, the lubrication behavior of motor oil with a small concentration (less than 10%) of pyro-oil in the hydrodynamics regime is not expected to be altered.

3.4. Wettability and Tribology

The wetting behavior of lubricating oils on steel surfaces impacts the tribological performance of any mechanical system. The current motor oils are generally mineral or petroleum oils which are formulated using several additives in order to improve their lubrication properties. Therefore, several adjustments of motor oils were made to achieve the best wettability behavior of oils on steel surfaces [22]. However, if new modifications were made to the chemical structure of the motor oil lubricant, then the chemical and physical interactions between the oil and the metal surface might not be shifted immediately. Therefore, if a new material is added to the motor oil, it is critical to study its effect on the wetting properties of the virgin motor oil.

This study explores the wettability property of ELT pyro-oil and motor oil at various temperatures. It also investigates the effect of adding different concentrations of pyro-oil to the wetting properties of motor oil. Typically, the wettability evaluation involves determining the contact angle (CA) as the main factor to identify the degree of wetting when a liquid and solid interact. In this investigation, the surface wettability was measured for the virgin motor oil and pyro-oil in addition to their mixture samples. Figure 8a shows that all samples exhibited a well-structured droplet at all examined temperatures. Figure 8b presents the variation in the CA of motor oil, pyro-oil, and their mixtures with temperature. In all examined temperatures, the pyro-oil was the lowest in CA, while the motor oil and the 10–90% oil mixture were the highest and almost similar in CA values. Also, for all oil samples, the temperature rise caused a minor rise in the CA value. Hence, it is clear that the addition of 10 wt.% of pyro-oil to the motor oil has no impact on the wettability properties of the motor oil.
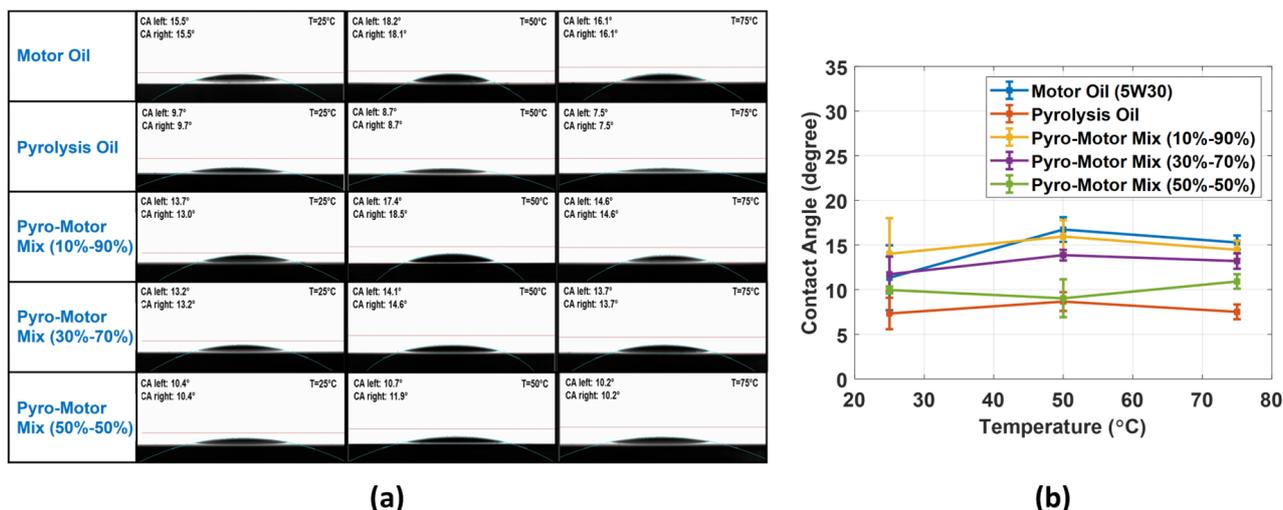
Figure 8. (**a**) Photos of the oil droplet depicting the CA at multiple temperatures for all samples. (**b**) Comparison of CA values against temperature for motor oil, pyro-oil, 10–90% oil mixture, 30–70% oil mixture, and 50–50% oil mixture.

The chemical, thermal stability, rheological, and wettability results clearly demonstrate that adding a small concentration (less than or equal to 10%) of pyro-oil to the motor oil will have almost no effect on the motor oil's performance. Therefore, the tribological study will include only pyro-oil, motor oil, and the 10–90% pyro-oil/motor oil mixture.

A tribological analysis of ELT pyro-oil oil and the 10–90% oil mixture was executed and compared to the virgin motor oil. In this investigation, different rotational speeds and operating temperatures were used to test the oil samples in order to identify their lubrication performance. Tribotests were executed using the MFT-5000 multi-function tribometer in a ball-on-disk setup. The applied normal load in all tribotests was set to 20 N, causing a maximum contact stress of 1300 MPa. Also, the speed varied from 0 to 1500 rpm to measure the COF under mixed and boundary lubrication conditions. Figure 9 shows the variation in the friction coefficient with the rotational speed for all examined oil samples at three operating temperatures. The transition from boundary lubrication to mixed lubrication is observed from the rapid decrease in COF values with increasing disk rotational speeds (see Figure 9). The obtained results revealed that the value of COF drops as the rotational speed increases for all oil samples, suggesting that the lubricating oil is functioning under mixed lubrication conditions. It is also noted that all examined oil samples had nearly similar COF values, especially at low speeds; however, at high speeds, the COF values start to slightly differ (see Figure 9). For the 25 °C operating temperature and at 1500 rpm speed, the value of COF for the motor oil was less than the pyro-oil and the 10–90% oil mixture by 25% and 11%, respectively. For the case of a 50 °C operating temperature and at 1500 rpm speed, the value of COF for the 10–90% oil mixture was less than the pyro-oil and the motor oil by 32% and 14%, respectively. At a 75 °C temperature and 1500 rpm speed, the value of COF for the motor oil and the 10–90% oil mixture were identical and less than the pyro-oil by 36%. These findings show that the 10–90% oil mixture has similar lubrication performance to the motor oil at nearly all examined temperatures and sliding speeds. The slight decrease in COF values of the pyro-oil/motor oil mixture is attributed to the reduction in the oil's viscosity with the increase in temperature, resulting in a lower shear force. Similar behavior was observed in a previous study [38] in the mixed lubrication; this was explained by the reducing interlaminar shear force that leads to lower COF values.
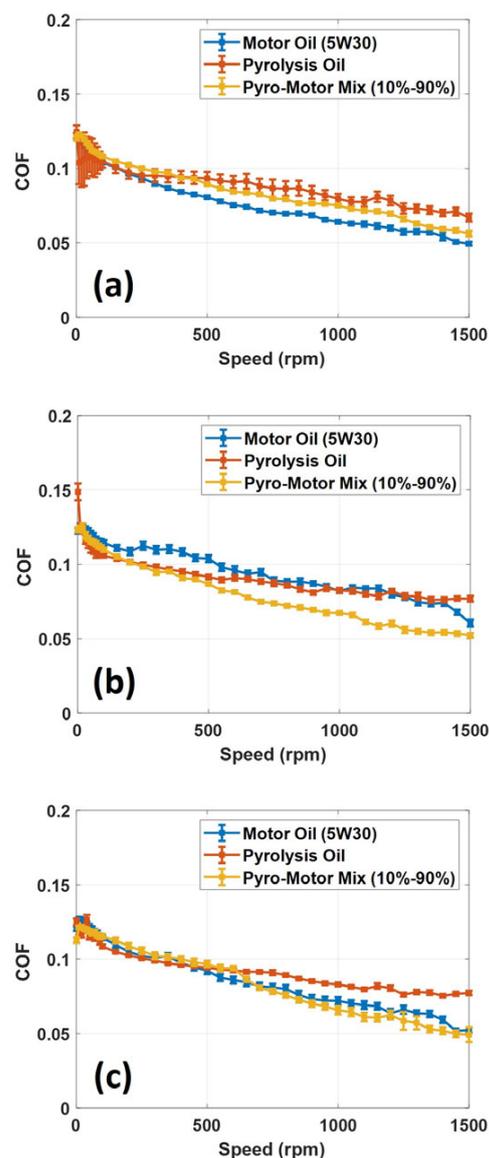
Figure 9. Variation in COF with speed for motor oil, pyro-oil, and the 10–90% oil mixture under operating temperatures of (**a**) 25 °C, (**b**) 50 °C, and (**c**) 75 °C.

After every tribotest, the wear scars on ball and disk specimens were analyzed to assess the lubricating properties of the investigated oils. Figure 10 depicts wear scar images on ball specimens after tribotesting at multiple operating temperatures using motor oil, pyro-oil, and the 10–90% oil mixture. It can be seen that the ball wear scars for the motor oil and the 10–90% oil mixture were nearly identical and smaller than the one for the pyro-oil under a 25 °C operating temperature (see Figure 10a). Nevertheless, after tribotesting under 50 °C and 75 °C operating temperatures, similar wear scars on the ball specimen were found for all tested oil samples (see Figure 10b,c). Measurements of the wear scar diameter on ball specimens were performed via an optical profilometer, while the volume of wear loss was determined as per ASTM-G99 [39] standards using the following equation:

$$\text{Ball volume loss} = \frac{\pi h}{6}\left[\frac{3d^2}{4} + h^2\right]$$

where

$h = r - \sqrt{r^2 - d^2/4};$

d = wear scar diameter;

r = ball radius.
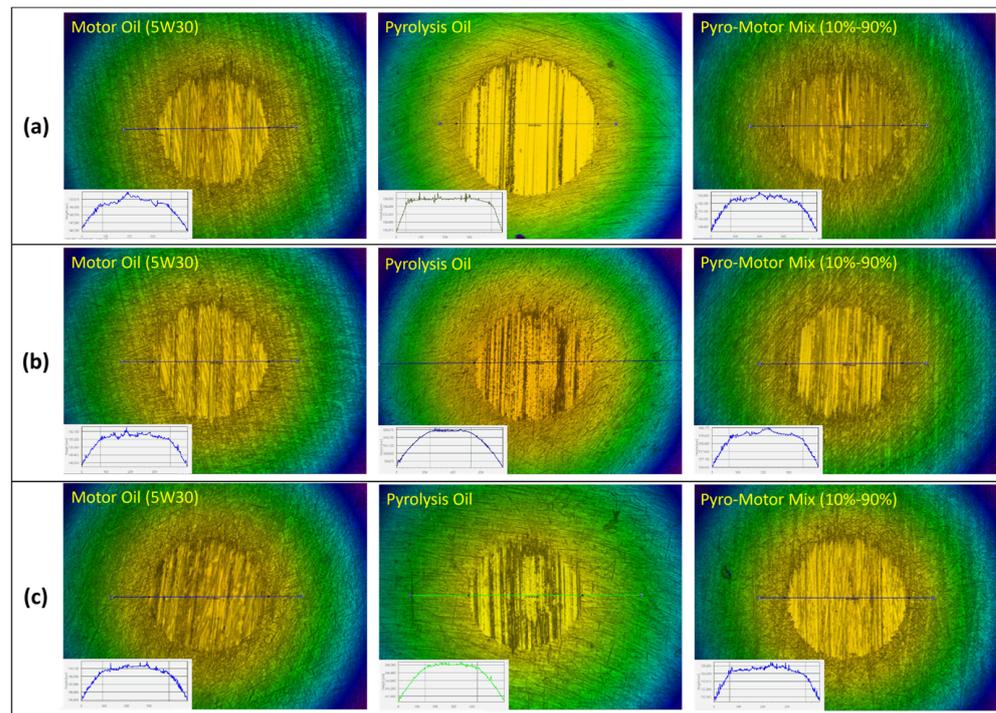
Figure 10. Images of wear scar of ball specimen after tribotesting using motor oil, pyro-oil, and 10–90% oil mixture samples under operating temperatures of (**a**) 25 °C, (**b**) 50 °C, (**c**) 75 °C. Inset: line profile across the wear scar.

Figure 11 presents the diameter of wear scars and calculated volume of wear loss of the ball after tribotesting at multiple operating temperatures using motor oil, pyro-oil, and the 10–90% oil mixture. For a 25 °C operating temperature, the motor oil and the 10–90% oil mixture had nearly similar wear scar diameters of 295 µm and 300 µm, whereas the pyro-oil resulted in a 345 µm diameter wear scar. Furthermore, the volume of wear loss of the ball specimen for the motor oil was less than the 10–90% oil mixture and the pyro-oil by 7% and 47%, respectively. Still, all oil samples had almost the same wear results under 50 °C and 75 °C operating temperatures.
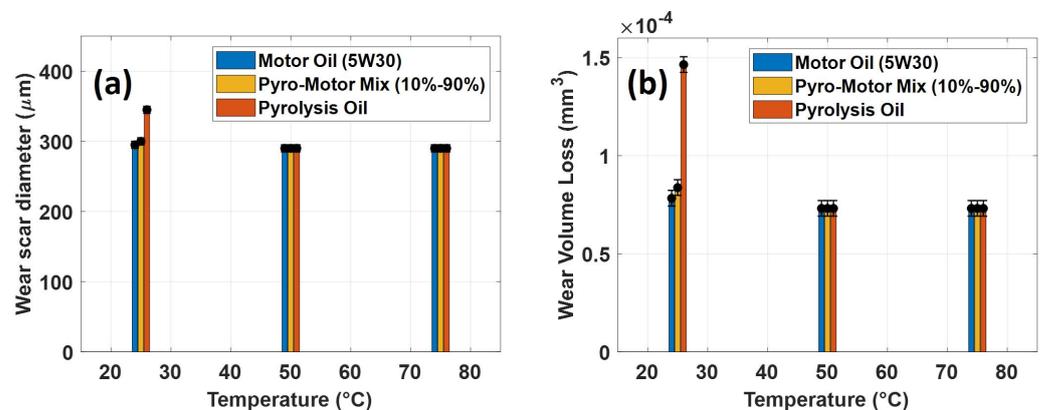
Figure 11. (**a**) Diameter of wear scar and (**b**) volume of wear loss of ball specimen after tribotesting using motor oil, 10–90% oil mixture, and pyro-oil samples under multiple operating temperatures.

Figure 12 depicts wear scars images on the disk specimen after tribotesting using motor oil, pyro-oil, and 10–90% oil mixture samples at different temperatures. For the case of the 25 °C operating temperature, the disk wear scar for the pyro-oil is clearly wider

and rougher in comparison to the motor oil and the 10–90% oil mixture (see Figure 12a). Conversely, for 50 °C and 75 °C operating temperatures, wear scars on the disk specimen were almost the same for all oil samples. An additional study was performed for disk wear scars by examining a surface line-height across each disk wear scar. The obtained results clearly indicate that the disk wear scars were very shallow, having a depth of lower than 100 nm for all examined oil samples and all operating temperatures. In brief, the obtained frictional and wear findings clearly indicate that adding a small concentration of pyro-oil (less than or equal to 10%) will not affect the lubrication functioning of existing motor oils.
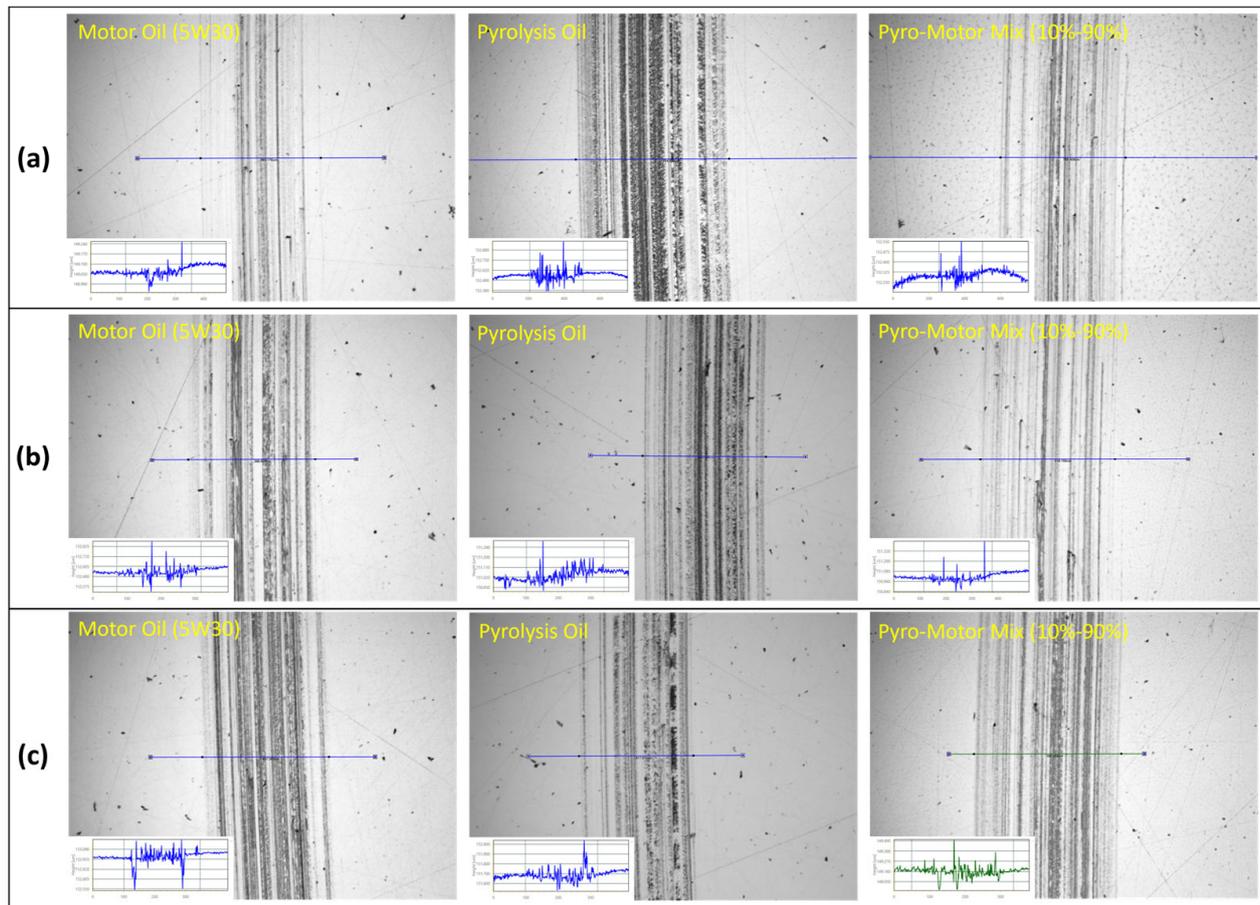
Figure 12. Images of wear scar of disk specimen after tribotesting using motor oil, pyro-oil, and 10–90% oil mixture samples under operating temperatures of (**a**) 25 °C, (**b**) 50 °C, (**c**) 75 °C. Inset: line profile across the wear scar.

3.5. Statistical and Regression Analysis

The statistical analysis of the tribotesting results presented in the former section was performed. A second-order polynomial model has been proposed to define the friction coefficient (*COF*) as a function of (a) rotational speed (*RPM*) in the range of 0 to 1500, (b) operating temperature in the range of 25 °C to 75 °C, and (c) percent of *pyrolysis oil* to motor oil ranging from 0% (i.e., motor oil) to 10%, to 100% (i.e., tire *pyrolysis oil*), as follows:

$$
\begin{aligned}
COF = {} & 0.1033 - \left(0.060 \times 10^{-3} \times RPM\right) + \left(0.651 \times 10^{-3} \times Temperature\right) - \left(0.386 \times 10^{-3} \times Pyro\ Oil\%\right) \\
& - \left(1.151 \times 10^{-7} \times RRM \times Temperature\right) + \left(1.619 \times 10^{-7} \times RPM \times Pyro\ Oil\%\right) \\
& + \left(2.749 \times 10^{-8} \times Temperature \times pyro\ Oil\ \%\right) + \left(1.556 \times 10^{-8} \times RPM^2\right) \\
& - \left(4.966 \times 10^{-6} \times Temperature^2\right) + \left(3.188 \times 10^{-6} \times (Pyro\ Oil\ \%)^2\right)
\end{aligned}
$$

Table 4 presents the model's fitness to the tribotests data with an R^2 of 0.9376, an adjusted R^2 of 0.9360, and an adequate precision number of 79. It is safe to assume that the obtained model has a great fit to the tribotests data.

Table 4. Fit statistics of the model.

Standard Deviation	0.0052
Mean	0.0910
Coefficient of variance (C.V. %)	5.70
R^2	0.9376
Adjusted R^2	0.9360
Predicted R^2	0.9341
Adequate Precision	79.0714

Figure 13 shows 3D surface figures generated using the obtained model that relates the COF with rotational speed and percentage of pyro-oil for different operating temperatures. It should be noted that the tribotests data in Figure 13 are presented as red and pink circles above and below, respectively, the 3D surface that represents the model-predicted COF values. In all examined operating temperatures, the COF increases with the increase in the percentage of pyro-oil and decreases as the speed increases. Moreover, as the percentage of pyro-oil increases from 0%, the COF starts to decrease up to around 10%; then, it starts to increase again, reaching maximum values at 100% pyro-oil (see Figure 13).
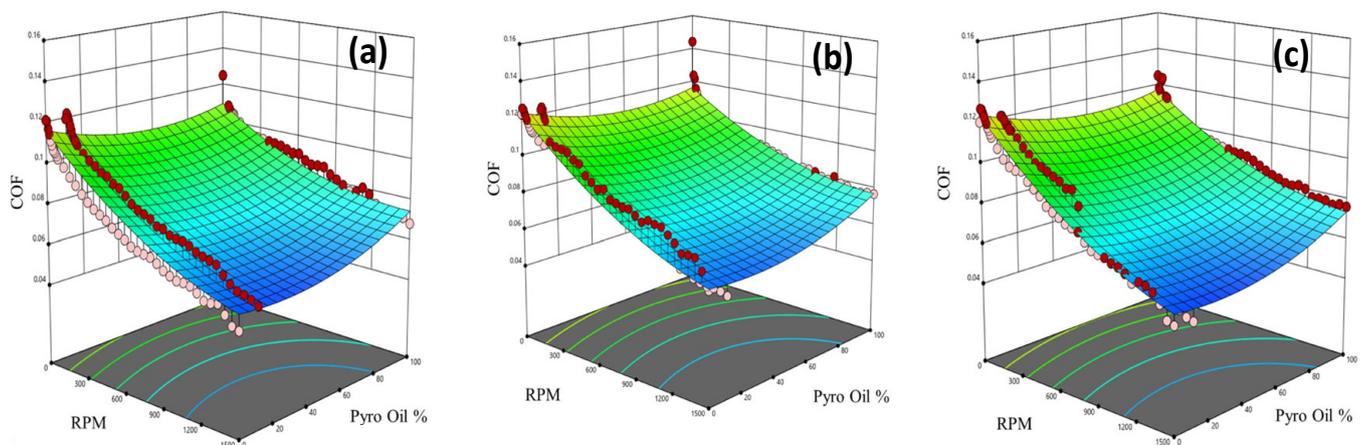
Figure 13. COF model (3D surface) and experimental data (red and pink circles) versus rotational speed and pyro-oil percent in motor oil under examined temperatures of (**a**) 25 °C, (**b**) 50 °C, and (**c**) 75 °C.

An Analysis of Variance (ANOVA) study was performed through an assessment of the mean values of three or more variables in order to conclude if a significant change occurs between them. In this study, an ANOVA test was performed to analyze the significance of the proposed model as well as the significance of its variables. Additional details on conducting and interpreting the ANOVA test results can be found in [40]. Table 5 shows that the model has a p-value under 0.05, which can be interpreted to mean that the model can be used to describe the experimental data. On the other hand, each variable shows a p-value under 0.05, which can be interpreted to mean that the variables used in this experiment have a statistically significant effect on the output, i.e., the friction coefficient. Similarly, all the interactions between the variables (except BC) show a p-value less than 0.05. Therefore, the main findings from the ANOVA test results are as follows: (a) the

developed model is statistically significant in characterizing the experimental tribotest data, and (b) the used variables (i.e., RPM, temperature, and pyro-oil %) have a statistically significant effect on the COF value.

Table 5. Outputs from ANOVA test on the significance of the proposed model and its variables.

Source	Sum of Squares	df	Mean Square	*F*-Value	*p*-Value	Results
Developed Model	0.1382	9	0.0154	569.58	$<10^{-4}$	significant
A-RPM	0.0817	1	0.0817	3031.29	$<10^{-4}$	significant
B-Temperature	0.0006	1	0.0006	22.00	$<10^{-4}$	significant
C-Pyro-Oil %	0.0017	1	0.0017	63.53	$<10^{-4}$	significant
AB	0.0005	1	0.0005	17.17	$<10^{-4}$	significant
AC	0.0044	1	0.0044	164.90	$<10^{-4}$	significant
BC	2.236×10^{-7}	1	2.236×10^{-7}	0.0083	0.9275	insignificant
A^2	0.0030	1	0.0030	109.65	$<10^{-4}$	significant
B^2	0.0008	1	0.0008	27.87	$<10^{-4}$	significant
C^2	0.0005	1	0.0005	19.63	$<10^{-4}$	significant
Residual	0.0092	341	0.0000		$<10^{-4}$	
Cor Total	0.1474	350				

3.6. Remarks on Environmental and Economic Impact

After studying the mixtures' chemical, thermal stability, rheological, wettability, and tribological properties, it has been shown that adding 10% of pyro-oil to motor oil will result in similar rheological and tribological behavior. On the other hand, using recycled ELTs to create an additive to motor oil brings economic and environmental benefits. On the environmental side, there will be less dependence on petroleum products to produce lubricating oil, since most lubricant-based fluids are acquired through refining processes of crude oil [41]. The estimates for global demand for petroleum-based oil lubricants exceed 41 million tons of crude oil, and reducing the demand for crude oil by 10% by adding pyro-oil can make a huge impact in terms of greenhouse gas emissions reductions and the exploitation of raw and non-renewable sources. It has been estimated that around 4 billion tires are currently stockpiled globally, and annually, almost one billion tons of tires are discarded worldwide [42,43]. Moreover, 5.26 million tons of pyro-oil can be produced from every one billion tons of tire waste [44]. It can be seen that adding 10% of pyro-oil to motor oil might bring environmental benefits; however, an in-depth life cycle analysis is necessary. On the economic side, the lubrication market size in 2020 was USD 115.86 billion and is anticipated to increase to USD 133.55 billion in 2028 [45]. This means that producing oil from the pyrolysis of ELTs for lubrication purposes will create a new stream of profits by selling ELTs to recycling facilities, reducing the size of landfills, and freeing up valuable land. However, after proving that the 10–90% pyro-oil/motor oil mixture can provide similar technical performance as the motor oil, it is crucial to conduct an in-depth life cycle cost analysis and a feasibility study to fully understand the economic implications and make informed decisions.

4. Conclusions

The presented work comprehensively studied the chemical, thermal stability, rheological, wettability, and lubrication properties of motor oil, tire pyro-oil, and their mixtures. The pyro-oil was shown to exhibit lower thermal stability, rheological, wettability, and tribological properties relative to the motor oil. Hence, the usage of pyro-oil as a fluid

lubricant will be limited to industrial practices with low operating temperatures and light loads. Furthermore, this work created and studied pyrolysis oil and motor oil mixtures at three concentrations of 10–90%, 30–70%, and 50–50%. The achieved outcomes revealed that the 10–90% pyro-oil/motor oil mixture has nearly similar rheological, tribological, wettability, and thermal stability behavior to the virgin motor oil. As a result, the 10–90% mixture represents a good candidate as an oil lubricant in most industrial applications. This investigation showed that adding low concentrations of pyro-oil ($\leq$10%) has almost no influence on the motor oil's properties. Consequently, their addition to the motor oil will not impact its performance and functionality in all lubrication regimes. Moreover, the process of adding pyro-oil to the motor oil can be significantly improved by performing it upstream during the manufacturing of motor oil lubricants to design and control several lubricant properties such as the sulfur content, viscosity, etc. The present study demonstrated that pyro-oil derived from recycled used tires can be scaled up for industrial applications, offering a feasible use for stockpiled used tires that pose serious environmental issues.

References

1. Kupareva, A.; Mäki-Arvela, P.; Grénman, H.; Eränen, K.; Sjöholm, R.; Reunanen, M.; Murzin, D.Y. Chemical characterization of lube oils. *Energy Fuels* **2013**, *27*, 27–34. [CrossRef]
2. Graziano, D.; Daniels, E. *Assessment of Opportunities to Increase the Recovery and Recycling Rates of Waste Oils*; Argonne National Lab. (ANL): Argonne, IL, USA, 1995.
3. Kupareva, A.; Mäki-Arvela, P.; Murzin, D.Y. Technology for Rerefining Used Lube Oils Applied in Europe: A Review. *J. Chem. Technol. Biotechnol.* **2013**, *88*, 1780–1793. [CrossRef]
4. Kajdas, C. Re-Refined Base Oils: Quality and Ecology. In Proceedings of the 4th European Rerefining Congress, Brussels, Belgium, 17 November 2009.
5. Dutta, S. Middle East lubricant suppliers seek market diversification: Expansion into new industrial sectors reduces dependence on crude oil. *Tribol. Lubr. Technol.* **2018**, *74*, 18.
6. Nagy, G.; Szabó, L.; Baladincz, J. Possibilities for processing of used lubricating oils-part 2. *MOL Sci. Mag.* **2010**, *2*, 66–72.
7. Emma, A.F.; Alangar, S.; Yadav, A.K. Extraction and characterization of coffee husk biodiesel and investigation of its effect on performance, combustion, and emission characteristics in a diesel engine. *Energy Convers. Manag. X* **2022**, *14*, 100214. [CrossRef]
8. Januszewicz, K.; Hunicz, J.; Kazimierski, P.; Rybak, A.; Suchocki, T.; Duda, K.; Mikulski, M. An experimental assessment on a diesel engine powered by blends of waste-plastic-derived pyrolysis oil with diesel. *Energy* **2023**, *281*, 128330. [CrossRef]

9. Al-Salem, S.M.; Antelava, A.; Constantinou, A.; Manos, G.; Dutta, A. A review on thermal and catalytic pyrolysis of plastic solid waste (PSW). *J. Environ. Manag.* **2017**, *197*, 177–198. [CrossRef]

10. Antelava, A.; Damilos, S.; Hafeez, S.; Manos, G.; Al-Salem, S.M.; Sharma, B.K.; Kohli, K.; Constantinou, A. Plastic solid waste (PSW) in the context of life cycle assessment (LCA) and sustainable management. *Environ. Manag.* **2019**, *64*, 230–244. [CrossRef]

11. Williams, P.T. Pyrolysis of waste tyres: A review. *Waste Manag.* **2013**, *33*, 1714–1728. [CrossRef]

12. Gehrke, I.; Schläfle, S.; Bertling, R.; Öz, M.; Gregory, K. Mitigation measures to reduce tire and road wear particles. *Sci. Total Environ.* **2023**, *906*, 166537. [CrossRef]

13. Zerin, N.; Rasul, M.; Jahirul, M.; Sayem, A. End-of-life tyre conversion to energy: A review on pyrolysis and activated carbon production processes and their challenges. *Sci. Total Environ.* **2023**, *905*, 166981. [CrossRef] [PubMed]

14. Al-Salem, S. Valorisation of end of life tyres (ELTs) in a newly developed pyrolysis fixed-bed batch process. *Process Saf. Environ. Prot.* **2020**, *138*, 167–175. [CrossRef]

15. Zhang, G.; Chen, F.; Zhang, Y.; Zhao, L.; Chen, J.; Cao, L.; Gao, J.; Xu, C. Properties and utilization of waste tire pyrolysis oil: A mini review. *Fuel Process. Technol.* **2021**, *211*, 106582. [CrossRef]

16. Hutchings, I.; Shipway, P. *Tribology: Friction and Wear of Engineering Materials*; Butterworth-Heinemann: Oxford, UK, 2017.

17. Holmberg, K.; Erdemir, A. The impact of tribology on energy use and CO_2 emission globally and in combustion engine and electric cars. *Tribol. Int.* **2019**, *135*, 389–396. [CrossRef]

18. Tonk, R. The science and technology of using nano-materials in engine oil as a lubricant additives. *Mater. Today Proc.* **2021**, *37*, 3475–3479. [CrossRef]

19. Gemsprim, M.S.; Babu, N.; Udhayakumar, S. Tribological evaluation of vegetable oil-based lubricant blends. *Mater. Today Proc.* **2021**, *37*, 2660–2665. [CrossRef]

20. Alazemi, A.A.; Alajmi, A.F.; Al-Salem, S.M. Investigation of Chemical, Physical, and Tribological Properties of Pyrolysis Oil Derived from End-of-Life Tires (ELTs) against Conventional Engine Oil. *Lubricants* **2024**, *12*, 188. [CrossRef]

21. Decote, P.A.; Negris, L.; Simonassi, P.; Druzian, G.T.; Flores, E.M.; Vicente, M.A.; Santos, M.F. Quality analysis of oil recovered from used locomotive engine oil using ultrasound-assisted solvent extraction. *Chem. Eng. Res. Des.* **2023**, *197*, 603–616. [CrossRef]

22. Alazemi, A.A.; Alzubi, F.G.; Alhazza, A.; Dysart, A.; Pol, V.G. Rheological and wettability properties of engine oil with a submicron spherical carbon particle lubricant mixture. *Int. J. Automot. Technol.* **2020**, *21*, 1475–1482. [CrossRef]

23. Pfeiffer, P.; Ronai, B.; Vorlaufer, G.; Dörr, N.; Filzmoser, P. Weighted LASSO variable selection for the analysis of FTIR spectra applied to the prediction of engine oil degradation. *Chemom. Intell. Lab. Syst.* **2022**, *228*, 104617. [CrossRef]

24. Aberoumand, S.; Jafarimoghaddam, A. Experimental study on synthesis, stability, thermal conductivity and viscosity of Cu–engine oil nanofluid. *J. Taiwan Inst. Chem. Eng.* **2017**, *71*, 315–322. [CrossRef]

25. Alazemi, A.A.; Etacheri, V.; Dysart, A.D.; Stacke, L.-E.; Pol, V.G.; Sadeghi, F. Ultrasmooth submicrometer carbon spheres as lubricant additives for friction and wear reduction. *ACS Appl. Mater. Interfaces* **2015**, *7*, 5514–5521. [CrossRef] [PubMed]

26. Stankovikj, F.; Tran, C.-C.; Kaliaguine, S.; Olarte, M.V.; Garcia-Perez, M. Evolution of functional groups during pyrolysis oil upgrading. *Energy Fuels* **2017**, *31*, 8300–8316. [CrossRef]

27. González, J.F.; Encinar, J.M.; Canito, J.L.; Rodríguez, J.J. Pyrolysis of automobile tyre waste. Influence of operating variables and kinetics study. *J. Anal. Appl. Pyrolysis* **2001**, *58*, 667–683. [CrossRef]

28. Menares, T.; Herrera, J.; Romero, R.; Osorio, P.; Arteaga-Pérez, L.E. Waste tires pyrolysis kinetics and reaction mechanisms explained by TGA and Py-GC/MS under kinetically-controlled regime. *Waste Manag.* **2020**, *102*, 21–29. [CrossRef]

29. Kadhim, A.; Al-Amiery, A. X-ray fluorescence of copper, nickle and zinc nanoparticles in motor oil prepared by laser treatment. *J. Adv. Res. Fluid Mech. Therm. Sci.* **2021**, *83*, 178–185. [CrossRef]

30. Abnisa, F.; Daud, W.M.A.W.; Sahu, J.N. Pyrolysis of mixtures of palm shell and polystyrene: An optional method to produce a high-grade of pyrolysis oil. *Environ. Prog. Sustain. Energy* **2014**, *33*, 1026–1033. [CrossRef]

31. Osayi, J.I.; Iyuke, S.; Daramola, M.O.; Osifo, P.; Van Der Walt, I.J.; Ogbeide, S.E. Evaluation of pyrolytic oil from used tires and natural rubber (*Hevea brasiliensis*). *Chem. Eng. Commun.* **2018**, *205*, 805–821. [CrossRef]

32. Mishra, A.; Kumari, U.; Turlapati, V.Y.; Siddiqi, H.; Meikap, B. Extensive thermogravimetric and thermo-kinetic study of waste motor oil based on iso-conversional methods. *Energy Convers. Manag.* **2020**, *221*, 113194. [CrossRef]

33. Mishra, A.; Siddiqi, H.; Sonowal, M.; Chatterjee, A.; Maiti, P.; Meikap, B. A cumulative study on pyrolysis of waste motor oil exploring the design and development of a fixed-bed laboratory scale setup with emphasis on process parameter optimization, COMSOL simulation and preliminary risk assessment. *Process Saf. Environ. Prot.* **2024**, *185*, 1219–1231. [CrossRef]

34. Williams, P.T.; Besler, S.; Taylor, D.T. The pyrolysis of scrap automotive tyres: The influence of temperature and heating rate on product composition. *Fuel* **1990**, *69*, 1474–1482. [CrossRef]

35. Chandran, M.; Rajamamundi, P.; Kit, A.C. Tire oil from waste tire scraps using novel catalysts of manufacturing sand (M Sand) and TiO_2: Production and FTIR analysis. *Energy Sources Part A Recovery Util. Environ. Eff.* **2017**, *39*, 1928–1934. [CrossRef]

36. Kalam, M.; Masjuki, H.; Cho, H.M.; Mosarof, M.; Mahmud, I.; Chowdhury, M.A.; Zulkifli, N. Influences of thermal stability, and lubrication performance of biodegradable oil as an engine oil for improving the efficiency of heavy duty diesel engine. *Fuel* **2017**, *196*, 36–46. [CrossRef]

37. Nik, W.W.; Ani, F.; Masjuki, H. Thermal stability evaluation of palm oil as energy transport media. *Energy Convers. Manag.* **2005**, *46*, 2198–2215. [CrossRef]

38. Ruan, H.; Zhang, Y.; Li, S.; Yang, L.; Wang, C.; Wang, T.; Wang, Q. Effect of temperature on the friction and wear performance of porous oil-containing polyimide. *Tribol. Int.* **2021**, *157*, 106891. [CrossRef]

39. *ASTM G99-17*; Standard Test Method for Wear Testing with a Pin-on-Disk Apparatus. ASTM International: West Conshohocken, PA, USA, 2017.

40. Montgomery, D.C. *Design and Analysis of Experiments*; John Wiley & Sons: Hoboken, NJ, USA, 2017.

41. Okoro, E.E.; Erivona, N.O.; Sanni, S.E.; Orodu, K.B.; Igwilo, K.C. Modification of waste tire pyrolytic oil as base fluid for synthetic lube oil blending and production: Waste tire utilization approach. *J. Mater. Cycles Waste Manag.* **2020**, *22*, 1258–1269. [CrossRef]

42. Mokhtar, N.M.; Omar, R.; Idris, A. Microwave pyrolysis for conversion of materials to energy: A brief review. *Energy Sources Part A Recovery Util. Environ. Eff.* **2012**, *34*, 2104–2122. [CrossRef]

43. Liu, L.; Cai, G.; Zhang, J.; Liu, X.; Liu, K. Evaluation of engineering properties and environmental effect of recycled waste tire-sand/soil in geotechnical engineering: A compressive review. *Renew. Sustain. Energy Rev.* **2020**, *126*, 109831. [CrossRef]

44. Islam, M.; Nahian, M. Improvement of waste tire pyrolysis oil and performance test with diesel in CI Engine. *J. Renew. Energy* **2016**, *2016*, 5137247. [CrossRef]

45. Sarkar, S.; Datta, D.; Deepak, K.S.; Mondal, B.K.; Das, B. Comprehensive investigation of various re-refining technologies of used lubricating oil: A review. *J. Mater. Cycles Waste Manag.* **2023**, *25*, 1935–1965. [CrossRef]